12WCEE 2000

TEMPORAL DEPENDENCE OF SEISMIC HAZARD IN JAPAN

Tadashi ANNAKA[1] And Harumi YASHIRO[2]

SUMMARY

We evaluated the instantaneous seismic hazard in Japan during the coming 20 years (2000-2019 A.D.), 50 years (2000-2049 A.D.), and 100 years (2000-2099 A.D.) by combining a seismic source model with temporal dependence of large earthquake occurrence and an attenuation model for peak ground motions and 5% damped acceleration response spectrum developed based on the JMA-87 type strong motion accelerograms. For representing the seismic activity we used two types of seismic sources: (1) fault source generating large characteristic earthquakes, and (2) background seismic source generating small and moderate earthquakes. Fault sources generating large characteristic earthquakes repeatedly were individually identified from historical earthquake and active fault data. Recurrence intervals for large characteristic earthquakes are modeled by a lognormal distribution. Background seismic sources generating small and moderate earthquakes were continuously defined along the upper planes of four plates in and near Japan: the Pacific plate, the Philippine Sea plate, the Eurasia plate, and the Okhotsk plate. The effects of focal depth and fault extent on ground motion are incorporated into the attenuation model. Seismic hazard maps showing the probabilities that the peak ground acceleration of 400 cm/s2 and the spectral acceleration of 400 cm/s2 at the natural period of 1.0 s will be exceeded in a future time period were demonstrated as examples.

INTRODUCTION

A probabilistic seismic hazard analysis is a technique that estimates the probability that various levels of earthquake-caused ground motions will be exceeded at a given location in a given future time period. A seismic source model defining the location, frequency, and size of earthquakes must be developed more realistically based on the progress of the knowledge of earthquake processes. For this purpose it becomes important to evaluate instantaneous seismic hazard by taking account of the temporal change of seismic activity. It is also important to develop an attenuation model including uncertainty based on the strong motion records obtained by recent large earthquakes. A seismic source model in Japan, which takes account of the temporal dependence of large earthquake occurrence, was proposed by Annaka and Yashiro(1998) and an attenuation model for peak ground motions and 5% damped acceleration response spectrum based on the JMA-87 type strong motion accelerograms was proposed by Annaka et al.(1997). In the present study we evaluated the instantaneous seismic hazard in Japan during the coming 20 years (2000-2019A.D.), 50 years (2000-2049A.D.), and 100 years (2000-2099A.D.) by combining the developed seismic source and attenuation models.

[1] *Tokyo Electric Power Services Co., Ltd., 3-3, Higashi-ueno 3-chome, Taito-ku, Tokyo, Japan*
EMail: annaka@tepsco.co.jp
[2] *The Tokio Marine & Fire Insurance Co.Ltd., 1-4, Nakase, Mihama-ku, Chiba, Japan*
EMail: HARUMI.YASHIRO@tokiomarine.co.jp

2. SEISMIC SOURCE MODEL

2.1 Seismic Source Zones

The islands of Japan lie mainly on the Eurasia and Okhotsk plates. The Pacific and Philippine Sea plates subduct beneath the islands towards the west-northwest and northwest, respectively. The seismic activity in and around Japan is controlled by the interaction of the four plates. For representing the seismic activity we used two types of seismic sources: (1) fault source generating large characteristic earthquakes, and (2) background seismic source generating small and moderate earthquakes.

Fault sources are active sources in which large characteristic earthquakes are assumed to occur repeatedly. Recurrence intervals are modeled by a lognormal distribution. Fault sources were individually identified from historical earthquake and active fault data. Background seismic sources are seismotectonic provinces in which small and moderate earthquakes are assumed to occur randomly with uniform frequency. The truncated Gutenberg-Richter model is used as an earthquake recurrence relationship. Background seismic sources were continuously defined along the upper planes of the four plates above.

The distribution of 28 fault source zones identified from the fault models of historical large earthquakes is shown in Figure 1. The fault parameters compiled mainly by Sato(1989) were used. Each seismic source zone is modeled as a rectangular plane in three-dimensional space. The latitude, longitude and depth of a reference point on the plane, the length and width of the plane, and the dip angle were determined. By representing seismic source zone as a rectangular plane it becomes easy to take account of earthquake fault extent as proposed by Annaka and Nozawa(1988).

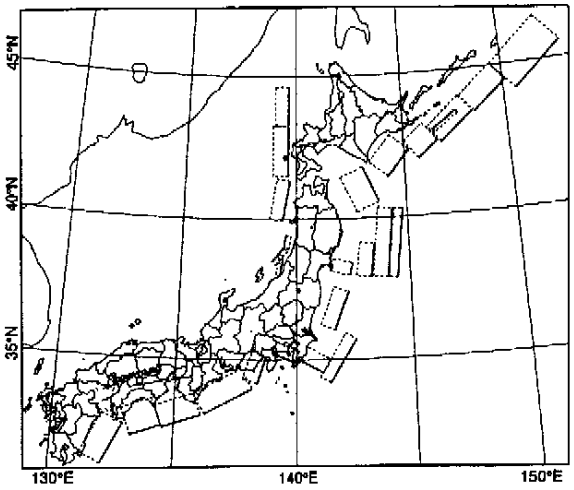

Figure 1: Fault source zones identified from historical earthquake data.

The distribution of 117 fault source zones identified from active faults whose lengths are greater than or equal to 20 km by Research Group for Active Faults of Japan(1991) is shown in Figure 2. Each seismic source zone is modeled as a rectangular plane or a multiple-segment line fault. A multiple-segment line fault is composed of straight lines.

The distribution of 36 background seismic source zones associated with the subducted Pacific plate is shown in Figure 3. Double-planed deep seismic zone is clearly observed for inter-mediate depth earthquakes along the subducted Pacific plate, so that the seismic source zones along the lower plane of the double deep seismic zone were modeled separately. The left and right maps in Figure 3 show the seismic source zones along the upper plane of the Pacific plate and those along the lower plane of the double deep seismic zone, respectively. Each seismic source zone is modeled as a rectangular plane, a triangle or a quadrangle. The depth is changed within a zone.

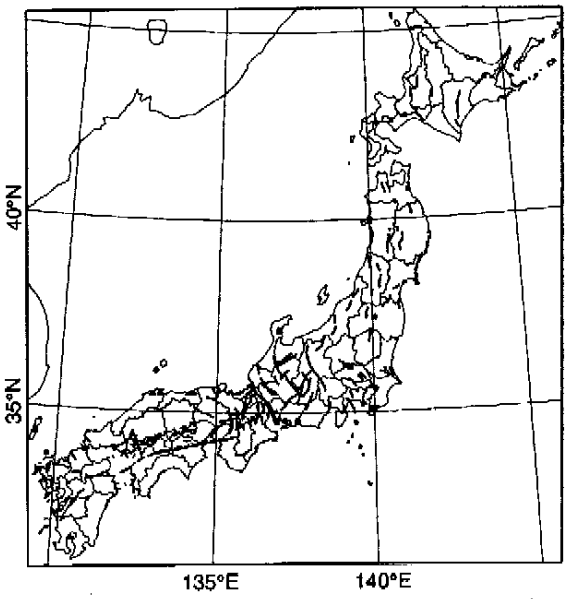

Figure 2: Fault source zones identified from active fault data.

The distribution of 29 background seismic source zones associated with the subducted Philippine Sea plate is shown in Figure 4. The geometry of the subducted Philippine Sea plate is more complicated than that of the Pacific plate.

The distribution of 23 background seismic source zones associated with the Eurasia and Okhotsk plates

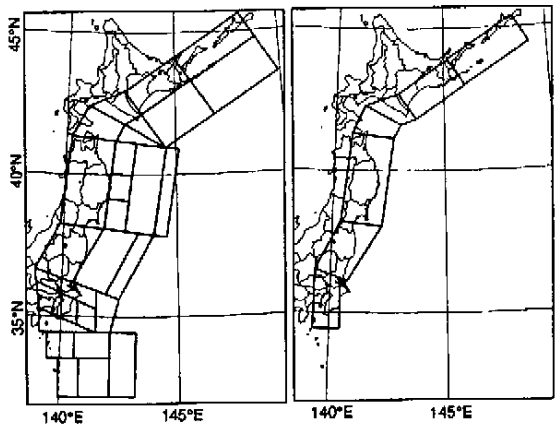

Figure 3: Background seismic source zones along the upper plane of the Pacific plate.

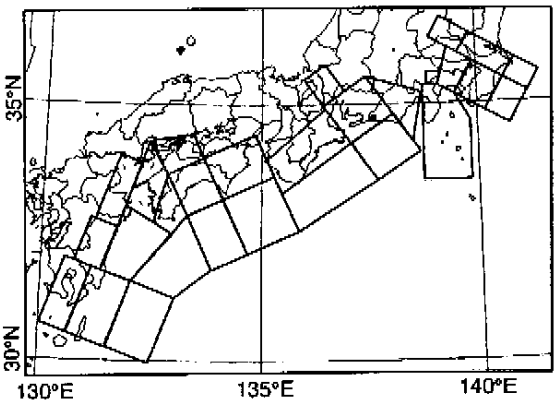

Figure 4: Background seismic source zones along the upper plane of the Philippine Sea plate

is shown in Figure 5. Most of the earthquakes occur in the upper crust with the thickness of about 15 km. Each seismic source zone is modeled as a polygon. The depth of the zones was fixed to be 5 km except one zone in the southern part of Hokkaido.

2.2 Seismicity Parameters

Seismicity parameters, which quantify the frequency and size of earthquakes that are expected to occur, must be determined for each seismic source zone. For fault sources the characteristic earthquake model by Youngs and Coppersmith(1985) was used. The parameters determined for them are as follows: (1) magnitude range of characteristic earthquakes, (2) magnitude-frequency relationships of characteristic earthquakes and their aftershocks, (3) mean and variability of recurrence intervals, and (4) the elapsed time since the most recent earthquake. For background seismic sources the truncated Gutenberg-Richter recurrence model was used. The a- and b- values of the Gutenberg-Richter relationship and maximum magnitude were determined for them.

The parameters of the fault source zones identified from historical earthquake data were determined mainly from the historical seismicity record. The bandwidth of 0.5 and the uniform distribution were usually used for the magnitude-frequency distribution of characteristic earthquakes. The evaluated recurrence intervals were in the range from 15 to 1,000 years. The cascade model proposed by WGCEP(1994) was applied for the large earthquakes along the Nankai trough. The parameters for the source zones along the Nankai trough are listed in Table 1. Occurrence rate is a mean value for a long time interval.

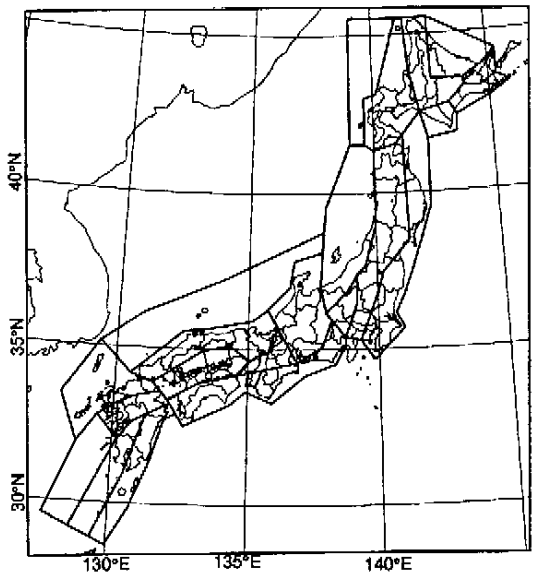

Figure 5: Background seismic source zones along the upper plane of the Eurasia and Okhotsk plates

Table 1: Parameters for source zones along the Nankai trough

Rupture Zone	Mw	Mj	Occurence Rate per 1,000 years	NAME
N1	8.1	7.6-8.0	3.845	Suruga-Wan
N2	8.4	7.9-8.3	3.845	Tokaido
N3+N4	8.5	8.1-8.5	5.127	Nankaido
N1+N2	8.5	8.0-8.4	1.282	Ansei-Tokai Type
N2~N4	8.7	8.1-8.5	0.0	
N1~N4	8.7	8.1-8.5	2.563	Hoei Type

The parameters of the fault source zones identified from active fault data were determined mainly from the geologic record. The magnitude range of characteristic earthquakes was evaluated based on the magnitude estimated from the fault length by the empirical relationship proposed by Matsuda(1975). The recurrence intervals for 23 active faults were determined from trenching surveys. The recurrence intervals for the other active faults were estimated from the degree of activity. The degree of activity of faults is classified as shown in Table 2 depending

Table 2: Classification of the degree of activity

Degree of Activity	Average Slip Rate (m/1,000 years)	Representative Value (m/1,000 years)
AA	5.6 - 18.0	10.0
A	1.8 - 5.6	3.16
AB	0.56 - 1.8	1.0
B	0.18 - 0.56	0.316
BC	0.056 - 0.18	0.01
C	0.01 - 0.056	0.0316

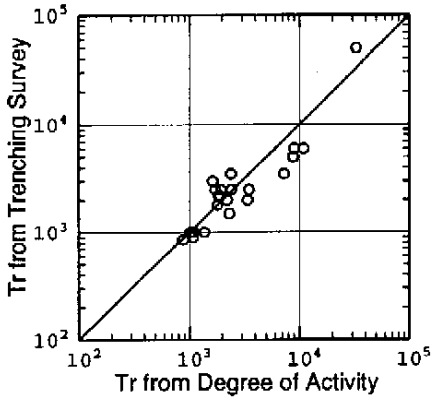

Figure 6: Comparison of recurrence intervals (Tr) obtained from trenching surveys with those calculated from the degree of activity.

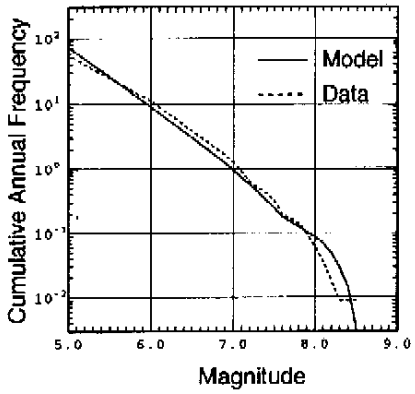

Figure 7: Comparison of magnitude-frequency distribution predicted for the proposed model with that observed from 1885 to 1997.

on the average slip rate.

The recurrence interval can be obtained from the ratio of the seismic moment release by a characteristic earthquake to the average rate of seismic moment release. Seismic moment versus fault length relationship proposed by Yamanaka and Shimazaki(1990) was used. Figure 6 shows the comparison of recurrence intervals from trenching surveys with those from the degrees of activity. The agreement of two recurrence intervals is good.

The parameters of the background seismic source were determined mainly from the earthquake data during the period from Jan. 1885 to July 1997. In order to evaluate the rate of independent earthquakes, dependent earthquakes (foreshocks, aftershocks, and earthquake swarm) were identified by their proximity in space and time and removed from the data. The b-values determined for four groups of seismic source zones range from 0.80 to 0.95. The a-value was determined from the number of earthquakes with magnitude greater than or equal to 6.0. The maximum magnitude was determined from historical earthquake data except the large characteristic earthquakes modeled as the fault sources.

Comparison of magnitude-frequency distribution predicted for the proposed seismic source model with that observed during the period from 1885 to 1997 is shown in Figure 7. The mean earthquake occurrence rate in and around Japan is well represented by the proposed model.

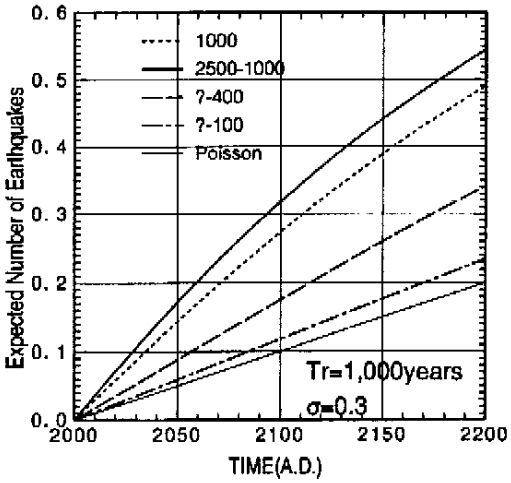

Figure 8: Comparison of expected number of earthquakes as a function of time estimated from varieties of information about the elapsed time since the most recent earthquake.

2.3 Temporal Change of Occurrence Rates

A renewal process model with a lognormal distribution of recurrence intervals was used. Varieties of inexact information on the age of the most recent earthquake as well as exact information were used for evaluating instantaneous earthquake

Table 3: Estimated earthquake occurrence rate per 1,000 years

Zone	Recurrence interval (years)	Last Rupture	Rate Poisson	Rate 2000-2019 σ=0.3	Rate 2000-2049 σ=0.3	Rate 2000-2099 σ=0.3	Rate 2000-2019 σ=0.5	NAME
J5	40	1978	25.00	30.52	26.09	25.55	28.70	Miyagi-oki
S1	200	1923	5.00	0.53	1.70	3.98	3.52	Sagami-Wan
S3	73	1923	13.70	31.67	19.38	16.64	21.40	Odawara
N1	130	1854	7.69	21.71	15.64	10.34	13.48	Suruga-Wan
N4	130	1946	7.69	1.97	5.49	7.70	6.66	Nankaido
N5	15	1984	66.67	79.89	70.31	67.37	72.49	Hyuganada
CB10	900	1200BP	1.11	4.41	4.15	3.75	2.27	Itoigawa-Shizoka T.L.
KK17	2471	1995	0.41	0.00	0.00	0.00	0.00	Rokko fault

occurrence rate based on a method proposed by Okumura et al.(1996).

Figure 8 shows the comparison of expected number of earthquakes as a function of time estimated from varieties of information. The mean and variability of recurrence intervals are assumed to be 1,000 years and 0.3 in natural logarithms, respectively. The results for four cases of information are compared with that for the Poisson process case. Case 1 (1000) is that the elapsed time since the most recent earthquake is 1,000 years. Case 2 (2500-1000) is that the elapsed time ranges from 2,500 years to 1,000 years. Case 3 (?-400) is that no other information except that no earthquakes occurred during the recent 400 years is available. Case 4 (?-100) is similar to Case 3 except that no earthquakes occurred during the recent 100 years. Expected number of earthquakes for Case 2 is the highest among all and the difference between Case 4 and Poisson is very small.

Using the renewal model and the available information on the most recent earthquakes, we estimated the expected numbers of large characteristic earthquakes for the fault source zones during the coming 20 years (2000-2019 A.D.), 50 years (2000-2049A.D.), and 100 years (2000-2099A.D.). Example of the result is shown in Table 3. Earthquake occurrence rates per 1,000 years are compared. The value of σ denotes the variability of recurrence intervals in natural logarithms.

3. ATTENUATION MODEL

An attenuation model for peak ground motions and 5% damped acceleration response spectrum proposed by Annaka et al.(1997) was used. The model is derived from the records of the JMA-87 type accelerometers obtained by the Japan Meteorological Agency (JMA) during the period from Aug.1, 1988 to Mar.31, 1996. The data set consists of 2085 pairs of orthogonal horizontal components from 388 earthquakes recorded at 77 JMA stations. The magnitudes and focal depths of the earthquakes are greater than or equal to 5.0 and less than 200 km, respectively. The shortest distances to the fault planes of the records are less than 500 km. The form of the regression equations is as follows:

$$\log A = C_m M + C_h H_C - C_d \log(R + 0.334\exp(0.663M)) + C_0 + \varepsilon \quad (1)$$

where A is the mean intensity of two horizontal components, M is JMA magnitude, H_C=H for H≦100km and H_C=100km for 100km<H<200km, H is the depth of the center of a fault plane of earthquake in km, and R is the shortest distance in km to the fault plane. Common logarithms are used. The constants, 0.334 and 0.663, are determined by the constraint that a peak ground acceleration becomes independent on magnitude when R reaches 0 km. The term ε is the error for the record and it can be represented by the sum of the two parts, $\varepsilon=\varepsilon_e+\varepsilon_o$, where ε_e and ε_o represent inter-event and intra-event variations, respectively. The ε_e and ε_o terms are assumed to be independent normally distributed variates with variances σ_e^2 and σ_o^2, respectively. The total variance σ^2 is equal to the sum of the two variances.

A two-stage regression method was used. The regression coefficients of the attenuation equations and the standard deviations of errors for peak ground motions (PGA: Peak Ground Acceleration, PGV: Peak Ground Velocity, and PGD: Peak Ground Displacement) are listed in Tables 4 and 5, respectively. The relations between regression coefficients and natural periods and those between standard deviations and natural periods for 5% damped acceleration response spectra are also shown in Figures 9 and 10, respectively. The constant C_0 was determined so that

Table 4: Coefficients of attenuation equations for peak ground motions

Index	C d	C m	C h	C o
PGA (cm/s2)	2.136	0.606	0.00459	1.730
PGV (cm/s)	1.918	0.725	0.00318	-0.519
PGD (cm)	1.635	0.935	0.00091	-2.992

Table 5: Standard deviations of errors for peak ground motions

Index	σ	σe	σo
PGA (cm/s2)	0.274	0.157	0.224
PGV (cm/s)	0.252	0.131	0.215
PGD (cm)	0.227	0.111	0.198

the attenuation equation can be applied to a site whose subsurface S wave velocity is about 400 m/s.

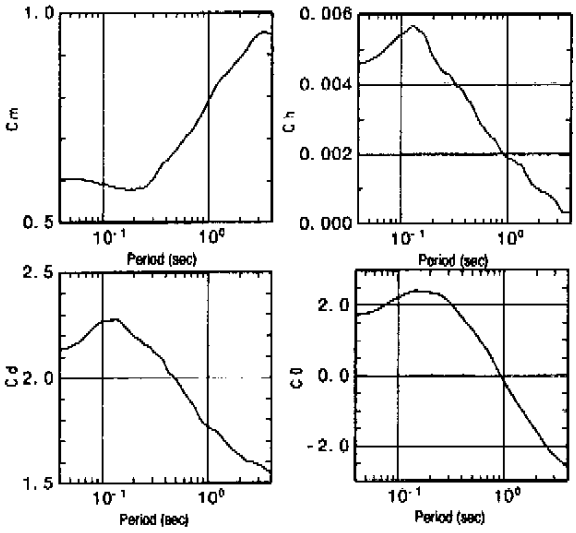

Figure 9: Relations between regression coefficients and natural periods for 5% damped acceleration response spectra

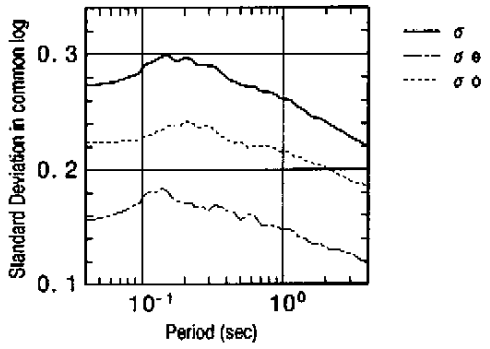

Figure 10: Relations between standard deviations of errors and natural periods for 5% damped acceleration response spectra

4. SEISMIC HAZARD MAPS

Using the seismic source model and the attenuation model above, we calculated the instantaneous seismic hazard curves during the coming 20 years (2000-2019 A.D.), 50 years (2000-2049A.D.), and 100 years (2000-2099A.D.) for 246 sites in Japan except the Ryukyu islands. The long-term seismic hazard curves based on the Poisson process were also calculated for comparison. The intervals of the sites are 0.5° both in latitude and longitude.

Seismic hazard maps showing the probabilities that the peak ground acceleration of 400 cm/s^2 and the spectral acceleration of 400 cm/s^2 at the natural period of 1.0 s will be exceeded during the coming 20 years, 50 years, 100 years, and the 20 years in case of the Poisson process are shown in Figures 11 and 12, respectively. Peak ground acceleration is nearly equal to 0.04 sec spectral acceleration. Probability of exccedance during the next 20 and 50 years is highest around the northern part of the Izu Peninsula. This reflects the higher occurrence rate for the Odawara earthquake and the Suruga-Wan earthquake (see Table 3). The probabilities along the Pacific coast of central Honshu and Shikoku in case of (a) are lower than those in case of (d). This is because the occurrence rate of the Nankaido earthquake is low during the coming 20 years (also see Table 3). The probabilities along the Pacific coast of Hokkaido, in central Honshu, and along the Pacific coast of central Honshu and Shikoku become higher as the period from the present becomes longer. The differences between Figures 11 and 12, which caused by variation in attenuation characteristics with natural periods, can be seen along the Pacific coast of northern Honshu, in central Kyushu, and so on.

5. CONCLUSIONS

Using a seismic source model with temporal dependence of large earthquake occurrence and an attenuation model developed based on the JMA-87 type strong motion accelerograms, we evaluated the instantaneous seismic hazard in Japan during the coming 20 years (2000-2019A.D.), 50 years (2000-2049A.D.), and 100 years (2000-2099A.D.). As for the seismic source model, the precise determination of the locations and geometries of the seismic source zones and the flexible framework for modeling the characteristics of seismic activity provide the firm basis for a future development of the model. The progress of the knowledge of earthquake processes may be easily incorporated into the model. As for the attenuation model, the effects of focal depth and fault extent on ground motion are properly taken into account and the nature of the error with natural period is revealed more clearly.

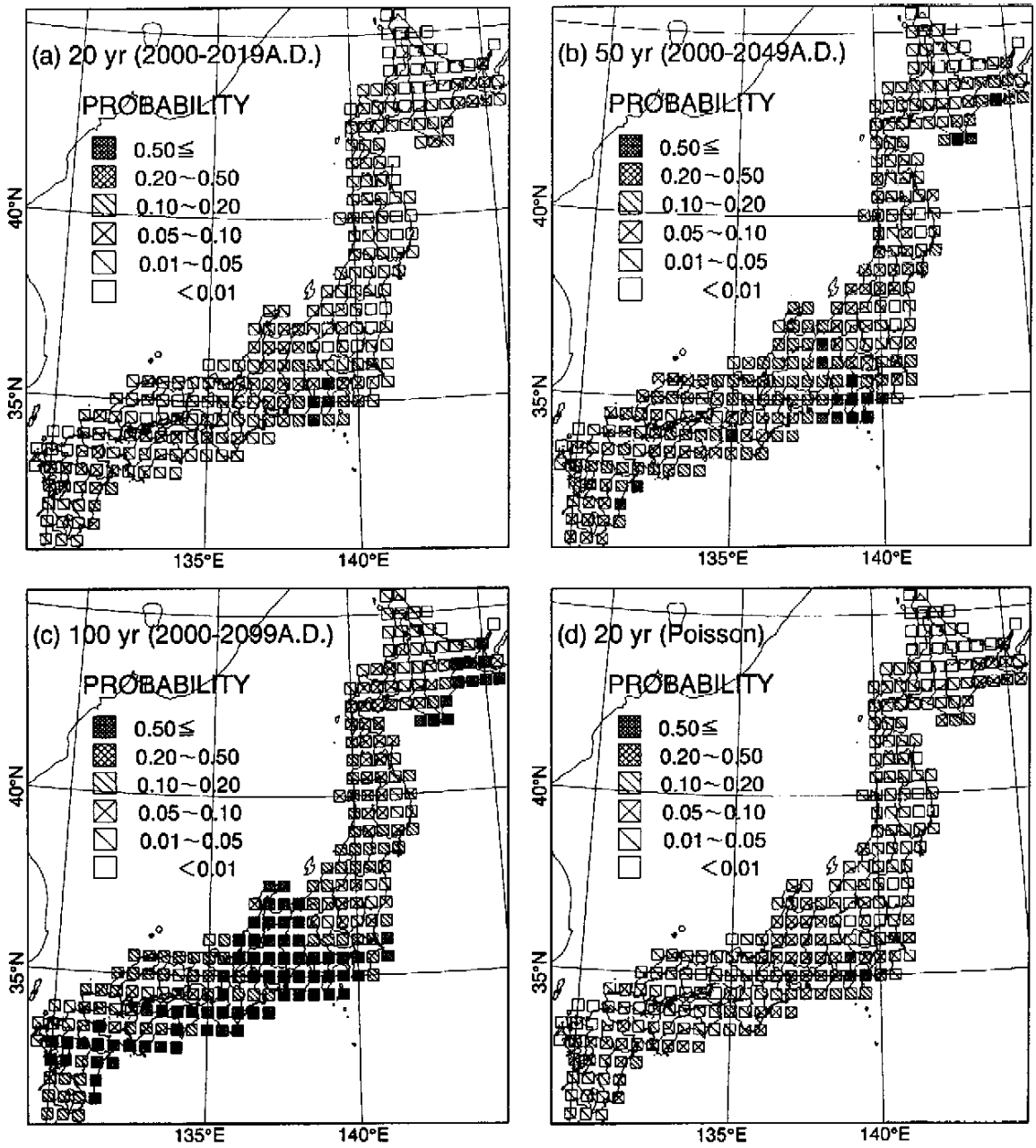

Figure 11: Seismic hazard maps showing the probabilities that the peak ground acceleration of 400 cm/s^2 will be exceeded during the coming (a) 20 years (2000-2019A.D.), (b) 50 years (2000-2049A.D.), (c) 100 years (2000-2099A.D.), and (d) the 20 years in case of the Poisson process

REFERENCES

Annaka, T. and Y. Nozawa(1988), "A probabilistic model for seismic hazard estimation in the Kanto district," *Proc. 9th World Conf. Earthquake Eng.*, II, pp. 107-112.

Annaka, T., F. Yamazaki, and F. Katahira(1997), "A proposal of an attenuation model for peak ground motions and 5% damped acceleration response spectra based on the JMA-87 type strong motion accelerograms", *Proceedings of the 24th JSCE Earthquake Engineering Symposium*, pp.161-164.(in Japanese)

Annaka, T. and H.Yashiro(1998), "A seismic source model with temporal dependence of large earthquake occurrence for probabilistic seismic hazard analysis in Japan", *Risk Analysis*, WITPRESS, Boston, pp.233-242.

Matsuda, T.(1975), "Magnitude and recurrence interval of earthquakes from a fault," *J. Seismol. Soc. Japan*, Ser.2, 28,pp. 269-283.(in Japanese)

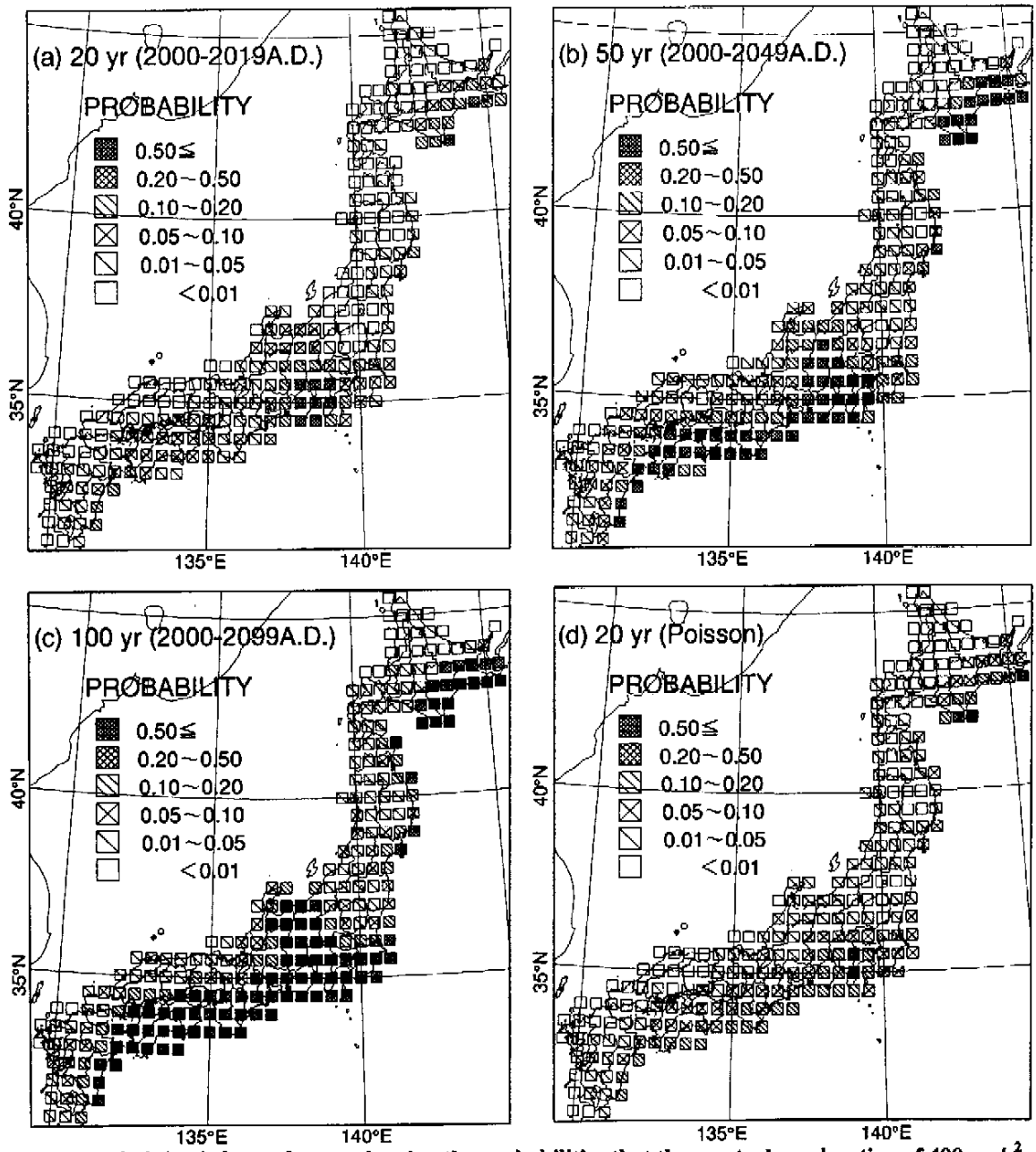

Figure 12: Seismic hazard maps showing the probabilities that the spectral acceleration of 400 cm/s^2 at the natural period of 1.0 s will be exceeded during the coming (a) 20 years (2000-2019A.D.), (b) 50 years (2000-2049A.D.), (c) 100 years (2000-2099A.D.), and (d) the 20 years in case of the Poisson process

Okumura, T., Y. Ishikawa, and H. Kameda(1996), "A method for evaluating the earthquake occurrence probability from active fault depending on information about the history of activity", *Proc. 51th Conf. JSCE*, I, pp. 498-499.(in Japanese)

Research Group for Active Faults of Japan(1991), *Active faults in Japan, sheet maps and inventories, Revised edition*, University of Tokyo Press, Tokyo, Japan.(in Japanese)

Sato, R.(1989), *Parameter handbook of earthquake faults in Japan*, Kazima Press, Japan.(in Japanese)

WGCEP(1995), "Seismic hazards in southern California, 1994 to 2024", *Bull. Seism. Soc. Am.*, 85, pp. 379-439.

Yamanaka, Y., and K. Shimazaki(1990), "Scaling relationships between the number of aftershocks and the size of the main shock", *J. Phys. Earth* 38, pp. 305-324.

Youngs, R. R. and K. J. Coppersmith(1985), "Implications of fault slip rates and earthquake recurrence models to probabilistic seismic hazard estimates", *Bull. Seism. Soc. Am.*, 75, pp. 939-964.